Received: 19 June 2019 | Accepted: 27 July 2019

DOI: 10.1111/jace.16720

ORIGINAL ARTICLE

Journal of the American Ceramic Society

Liquid and amorphous states of boron subarsenide

Murat Durandurdu

Department of Materials Science & Nanotechnology Engineering, Abdullah Gül University, Kayseri, Turkey

Correspondence
Murat Durandurdu, Department of Materials Science & Nanotechnology Engineering, Abdullah Gül University, Kayseri, Turkey.
Email: murat.durandurdu@agu.edu.tr

Funding information
Scientific and Technological Research Council of Turkey (117M372)

Abstract

Ab initio molecular dynamics simulations are executed to probe the short-range order and the electrical features of the liquid and amorphous boron subarsenide ($B_{12}As_2$). A drastic volume swelling of ~40% is witnessed for the liquid state, relative to the crystal. The density of the melt is found to be close to that of liquid boron. As the temperature applied is gradually decreased, the volume progressively decreases and a glass-transition zone at around 1400 K is observed. About 14% volume expansion is perceived for the amorphous phase. Due to the drastic density (volume) difference between the liquid and amorphous forms, their atomic structure is found to be different from each other. In the liquid phase at 2500 K, the mean coordination number (CN) of B and As atoms is 4.4 and 2.5, correspondingly. During the solidification process, both average CNs steadily increase and reach values of 5.5 (B-atom) and 4.14 (As-atom) at 300 K. The pentagonal pyramid-like motifs barely survive at 2500 K but during the quenching process they develop progressively and some of which lead to the formation of B_{12} clusters. In the amorphous state, the chain-like and A7-like As-As clusters are observed. Nonetheless, the noncrystalline state is proposed to be partially similar to the crystalline structure. The liquid state shows a metallic character while the amorphous form presents a semiconducting nature having an energy band gap much smaller than that of the crystalline phase.

KEYWORDS

amorphous, arsenic/arsenic compounds, atomistic simulation, first principles theory, glass-ceramics

1 | INTRODUCTION

Boron subarsenide ($B_{12}As_2$), a member of III-V semiconductors, has a wide forbidden energy band gap of 3.2 eV. Similar to most boron-rich compounds, because of its strong chemical bonding, it possesses remarkable features, for instance, high hardness, excellent electrical properties, and a high melting temperature.[1,2] Yet relative to other boron-rich compounds, $B_{12}As_2$ offers some additional advantages. Firstly, it has a high hole mobility, which might lead to a high current carrying capability.[3,4] Secondly it offers ability to self-heal from radiation damage. It shows no signs of damage even after electron bombardment. The combination of all these remarkable properties makes $B_{12}As_2$ a technologically important material having a wide range of suitable high tech applications, in particular, in harsh environments.[5]

The $B_{12}As_2$ compound has a rhombohedral crystal structure. In the crystal, As atoms form As-As bonds parallel to the axis of the primitive cell [111]. Raman spectroscopy studies[6,7] reported that $B_{12}As_2$ transforms to a distorted structure at 80-85 GPa. This phase transition is proposed to be the result of a robust distortion of the icosahedral structure. In spite of the strong deformation, the phase transition was found to be reversible. That is, by releasing the pressure, the original crystal structure was recovered again. In the X-ray diffraction investigations up to 25 GPa,[8] an anisotropy was detected in the compressibility of the crystal and c-axis was found to be more compressible than the other axes. In the same study,

its Bulk modulus was determined as 216 GPa. On the other hand, in the X-ray diffraction study performed up to 47 GPa,[5] the previous X-ray study was questioned due to the pressure-transmitting medium used. In the second X-ray study, Bulk module was reported to be about 150 GPa.[5] The theoretical studies estimated Bulk module to be approximately 181 and 197 GPa.[9,10]

In the literature, an experimental investigation reported the existence of an amorphous form of B_6As ($B_{13}As_2$) that was fabricated by conventional atmospheric pressure chemical vapor deposition in a hot-wall tube reactor.[11] The local structure and the properties of this material are still not established yet.

When the liquid structure of $B_{12}As_2$ is considered, to our knowledge, no study has been performed so far. In the present work, we examine, using ab initio molecular dynamics (MD) simulations, both atomic structure and electrical properties of $B_{12}As_2$ in its liquid and amorphous states and compare them with the crystalline phase. We reveal that the amorphous and liquid states exhibit a different local structure and electrical properties. The short-range order of the liquid phase does resemble neither that of amorphous configuration nor that of the crystal. Yet the noncrystalline form has a microstructure, partially similar to that of the crystal. Their electrical properties are different as well. The amorphous configuration is semiconductor but the amorphization causes a drastic band closure while the melt is metal.

2 | METHOD

We used an ab initio method[12] within the pseudopotential scheme[13] and a generalized gradient approximation.[14,15] We chose the double-zeta basis set and performed the Brillouin zone sampling only at Γ point. The NPT ensemble was preferred to accomplish the MD simulations. Single MD time step was set as 1.0 fs. We adopted the B_6O melt having 224 atoms as our starting structure and replaced O-atoms by As atoms. The initial configuration was exposed to a temperature of 2500 K for 40.0 ps. After a well-equilibrated melt was obtained, the system was cooled to 300 K in about 100 ps. We used the ISAACS[16] and VESTA[17] software to achieve some information regarding the $B_{12}As_2$ systems.

3 | RESULTS

The dynamics of the liquid state is considered by computing the mean-square displacement (MSD). Figure 1 shows the computed MSD. Beyond 40 fs, the MSD exhibits a linear behavior, representing a diffuse state in the liquid $B_{12}As_2$. From a linear fit from 60 to 900 fs and using the Einstein's relation $\left\langle (r(t)-r(0))^2 \right\rangle = 6tD$, the diffusion coefficient D is

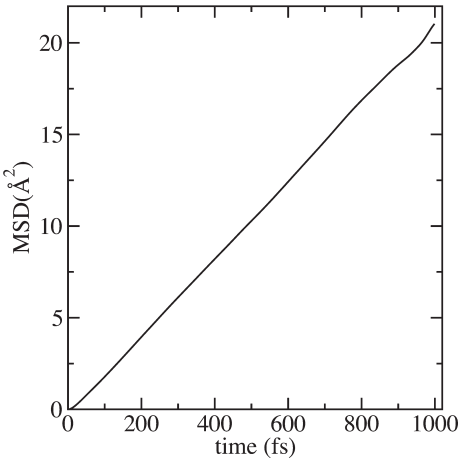

FIGURE 1 Mean-square displacement at 2500 K

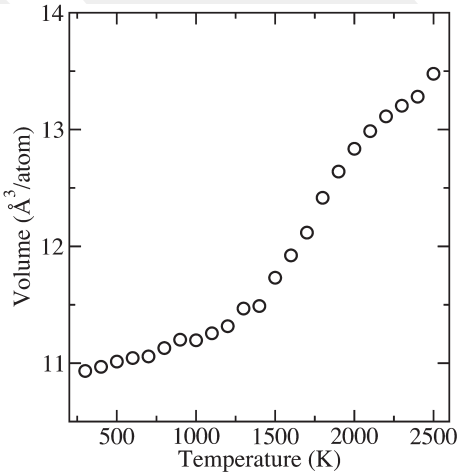

FIGURE 2 Temperature dependence of the volume per atom

projected to be ~3.5×10^{-4} cm^2/s. These finding means that 2500 K is high enough to have a liquid state of $B_{12}As_2$ in the simulation.

Figure 2 illustrates the temperature dependence of the volume per atom during the rapid solidification process. The volume shows a steady decrease with a faster rate between 2500 and 1400 K and a slower rate below 1400 K. The change in the slope of the temperature-volume curve at 1400 K is inferred as a glass-transition temperature (T_g) at around 1400 K. At room temperature, the volume of the amorphous state is 10.93 Å^3/atom (corresponding density is 3.03 g/cm^3), which is larger than 9.57 Å^3/atom (3.46 g/cm^3) estimated for the crystal. So accompanied by amorphization, a noticeable volume swelling of about 14% occurs in $B_{12}As_2$. The volume expansion for the liquid phase (V = 13.47 Å^3/atom and ρ = 2.46 g/cm^3) is even more drastic and about 40%, relative to the crystal.

In order to understand the temperature dependence of the atomic structure of the $B_{12}As_2$ system during the quenching process, it is indeed required to probe the partial pair

correlation functions (PPCFs). Some of which are provided in Figure 3. Those of the crystalline form are also plotted in the figure for the compression purpose. As expected, with decreasing temperature, the first peaks become sharper and their intensity increases, which are due to the formation of more ordered configurations in the system. The B-B, B-As and As-As bond lengths of the $B_{12}As_2$ crystal are estimated to be 1.79, 2.01, and 2.44 Å, correspondingly, which are fairly analogous to the experimental values of 1.74-1.90 Å (B-B), 1.99 Å (B-As), and 2.38 Å (As-As) (Ref. [18]) and the theoretical results of 1.71-1.87 Å (B-B), 1.97 Å (B-As), and 2.33 Å (As-As) (Ref. [10]). One can notice that the first neighbor separation of all pairs of the disordered states is different than that in the crystal. The first peak of As-As pair is located at 2.39 Å (2500 K) and 2.55 Å (300 K). So an expansion is observed in this separation by amorphization. In our earlier investigation on amorphous As, the As-As distance was estimated to be 2.56 Å, fairly close to the value predicted in the present work. Additionally this bond length is comparable with the first neighbor distances of 2.52 and 2.54 Å in the rhombohedral A7 crystal and liquid As, respectively.[19] The mean B-As bond distance is predicted to be 2.06 Å (liquid) and 2.11 Å (amorphous). Again an enlargement is detected in this bond separation by amorphization. The first peak position of B-B correlation is at 1.68 Å (liquid) and 1.77 Å (300 K). So one can see that relative to the crystalline state, amorphization leads to a decrease in the B-B bond distance, in a contrast to the other bond separations.

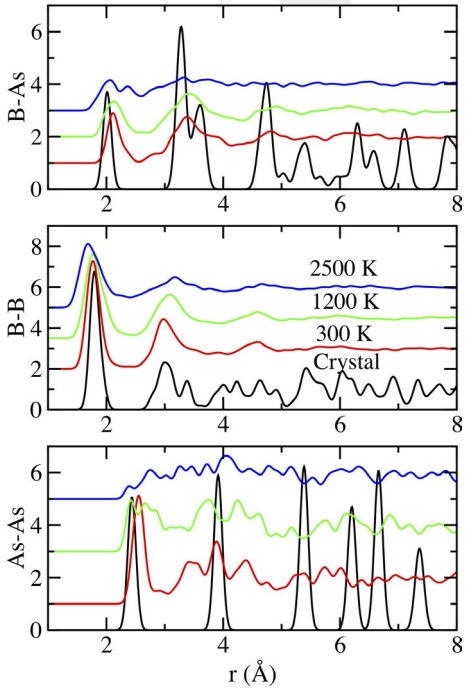

FIGURE 3 Partial pair correlation functions [Color figure can be viewed at wileyonlinelibrary.com]

In order to shed additional lights on of the microstructure of the $B_{12}As_2$ system, we probe the mean coordination numbers (CNs) and the coordination and chemical distributions at each temperature using the first minimum of the PPCFs as cutoff radii. Figure 4 shows the temperature dependence of the average B and As CNs. Both mean CNs do considerably change with temperature: they have a tendency to increase progressively with decreasing temperature. The mean CN of B-atoms is about 4.14 at 2500 K and becomes about 5.5 at room temperature. The average CN of As atoms is ~2.5 at 2500 K and reaches to ~3.6 at 300 K. So the mean CNs of the amorphous form are marginally less than those (6 for B-atoms and 4 for As-atoms) of the crystal. Yet as for the melt, they are considerably far from the CNs of the $B_{12}As_2$ crystal. Subsequently the average CN of both species is lower in the amorphous and liquid states than in the crystalline structure.

In the crystal, the B-B, B-As, As-B, and As-As CNs are 5.5, 0.5, 3.0, and 1.0, correspondingly. On the other hand, in the amorphous model, they are 5.06, 0.41, 2.5, and, 1.12, respectively. These findings suggest the formation of more As-As bonds and less the other bonds in the amorphous configuration.

As shown in Figure 5 and Table 1, B-atoms have a coordination distribution ranging from 2 to 8. At 2500 K, the threefold- to fivefold-coordinated configurations are the most

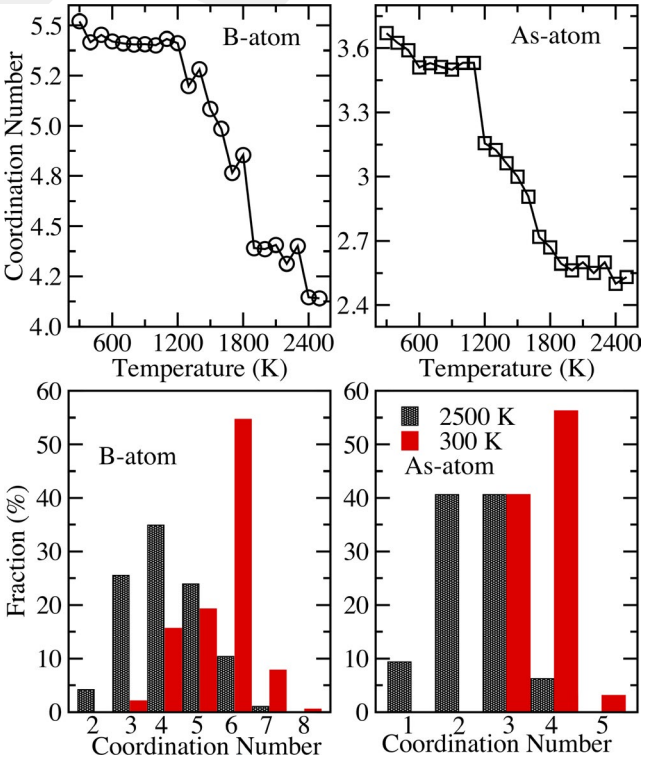

FIGURE 4 Temperature dependence of the average B and As coordination numbers and coordination distribution of B and As atoms at 2500 and 300 K [Color figure can be viewed at wileyonlinelibrary.com]

favorable ones. Their fraction ranges from ~24% to ~35%. The sixfold coordination barely exists in the liquid phase. On the other hand, in the amorphous form, the sixfold- and fivefold-coordinated motifs are the most privileged ones having frequencies of ~55% and ~19%, respectively. For the As-atoms, the twofold- and threefold-coordinated clusters are the most common clusters formed in the liquid state while the threefold- and fourfold-coordinated arrangements are the leading ones at room temperature.

The chemical distribution analysis provided in Table 1 offers extra information about the short-range order of the $B_{12}As_2$ systems. In the crystalline structure, the environment of B-atoms is represented by two type configurations; B-B_6 and B-B_5As while that of As atoms is represented by only one type motif; As-B_3As. Such kinds of arrangements are scarcely observed in the liquid state. On the other hand, B-B_6 and B-B_5As type clusters are the two leading motifs in the amorphous model. The fraction of As-B_3As type motif is only 18.75%. This analysis suggests that (a) the liquid state presents a quite different microstructure than the crystal and amorphous forms; and (b) the short-range order of B-atoms in the amorphous model is partially similar to that of the crystal whereas that of As-atoms in the noncrystalline state is incomparable with that of the crystalline state.

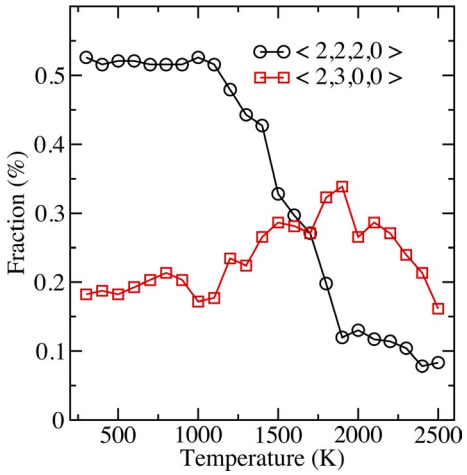

FIGURE 5 Temperature dependence of $\langle 2,2,2,0\rangle$ and $\langle 2,3,0,0\rangle$ polyhedrons [Color figure can be viewed at wileyonlinelibrary.com]

The Voronoi polyhedra analysis is carried out to resolve the nature of clusters formed around B-atoms. A Voronoi polyhedron is denoted by the indices $\langle l_3, l_4, l_5, l_6, \ldots\rangle$, here l_i is the number of i-edge faces of a cluster and $\sum l_i$ is CN. As expected, the crystal has only a pentagonal pyramid-like motif represented by $\langle 2,2,2,0\rangle$ index. During the rapid solidification process, we trace the variation of this cluster. Additionally we trace the change in the fraction of incomplete pentagonal-like motif represented by $\langle 2,3,0,0\rangle$ index. Figure 6 shows the temperature dependence of these two polyhedrons. At 2500 K, the fraction of the $\langle 2,2,2,0\rangle$ and $\langle 2,3,0,0\rangle$ types of motifs is about 8% and 16%, respectively. This observation means that pentagonal pyramids and hence B_{12} molecules do not survive in the liquid state. As the applied temperature is decreased, more $\langle 2,2,2,0\rangle$ type configurations develop drastically between 1900 and 1100 K and its frequency reaches a value of about 53% at 1100 K and below. In the amorphous state, nonnegligible amount of $\langle 2,3,0,0\rangle$ type of cluster exists as well. During the quenching process, the first complete B_{12} molecule develops at 1800-1700 K.

TABLE 1 Chemical identities around B and As atoms at 2500 K and 300 K

2500 K				300 K			
B		**As**		**B**		**As**	
B_4	21.87%	B_2	40.62%	B_6	37.50%	B_2As_2	28.12%
B_5	17.18%	B_3	21.87%	B_5As	16.66%	B_3As	18.75%
B_3	15.62%	B_2As	18.75%	B_5	11.45%	B_3	15.62%
B_3As	9.375%	B	6.250%	B_4As	7.812%	B_2As	15.62%
B_6	6.771%	B_4	3.125%	B_4	7.292%	B_4	9.375%
B_4As	6.250%	B_5	3.125%	B_7	6.250%	BAs_2	6.250%
B_2As	6.771%	As	3.125%	B_3As	5.208%	As_3	3.125%
B_5As	5.208%	B_3As	3.125%	B_2As_2	2.604%	B_5	3.125%
B_2As_2	2.604%			B_2As	2.083%		
B_2	3.125%			B_3As_2	1.042%		
B_7	2.083%			B_3	0.521%		
BAs_2	1.042%			B_8	0.521%		
BAs_3	0.521%			BAs_3	0.521%		
B_6As	0.521%			B_4As_2	0.521%		
B_7As	0.521%						
BAs	0.521%						

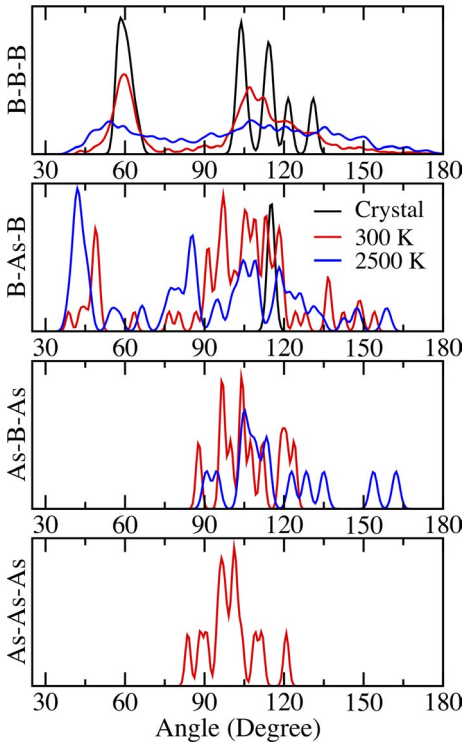

FIGURE 6 Bond angle distribution functions [Color figure can be viewed at wileyonlinelibrary.com]

The microstructure of $B_{12}As_2$ systems is additionally analyzed by the bond angle distribution functions (BADFs). Figure 7 illustrates the BADFs of the liquid, amorphous and crystalline structures of $B_{12}As_2$. The main difference between the ordered and disordered structures is the presence of As-As-As and As-B-As angles in the liquid and/or amorphous states. Such angles indicate some structural differences among these phases. The As-As-As angles have a distribution with two main peak located at 96° and 101°, which are indeed close to 97° formed in the A7 structure. By visualizing the amorphous model, we observe the formation of chain-like and A7-like clusters for As-atoms in the amorphous model (see Figure 8). The As-B-As angles range from 90° to 160°. The B-As-B angles in the crystal lead to a single peak at about 115°. In the disordered states, the angles produce a broad distribution ranging from 42° to 160°. The B-B-B distribution of the crystal presents angles at around 60°, 108°, 115°, 120°, and 130°. The first two angles are due to the intra-B_{12} molecules bonds while the others are a result of the inter-B_{12} clusters bonds. These angles are roughly presented in the amorphous model. The bond angle analysis suggests some resemblances around B atom and some distinctions around As atoms in the amorphous and crystalline phases.

The total density of states (TDOS) and partial density of states (PDOS) are computed to reveal the electronic structure of the $B_{12}As_2$ systems. Figure 8 gives the TDOS and PDOS calculated for the liquid, amorphous, and crystalline phases. The crystalline form has a clear forbidden gap of 2.96 eV,

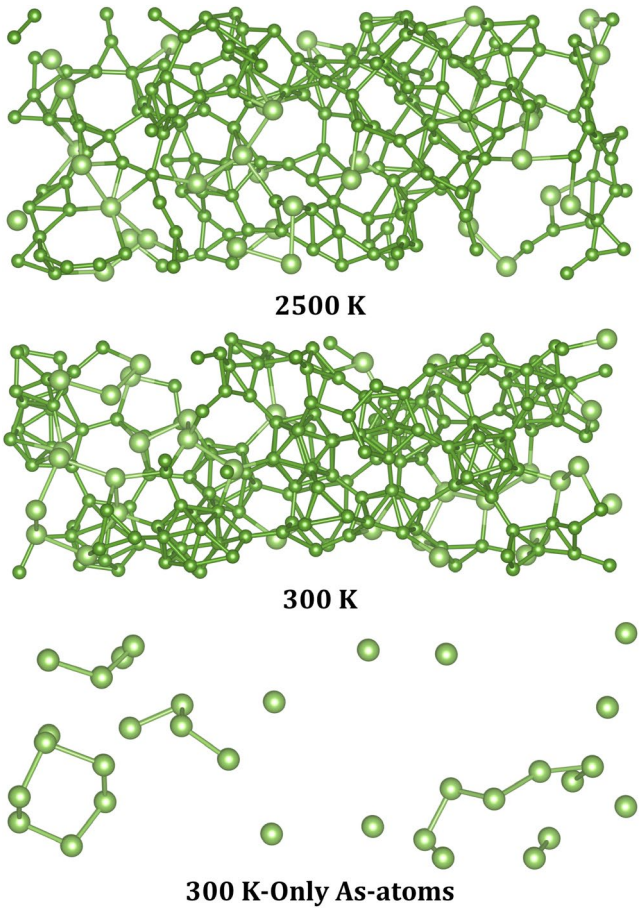

FIGURE 7 Ball-stick representation of $B_{12}As_2$ at 2500 and 300 K [Color figure can be viewed at wileyonlinelibrary.com]

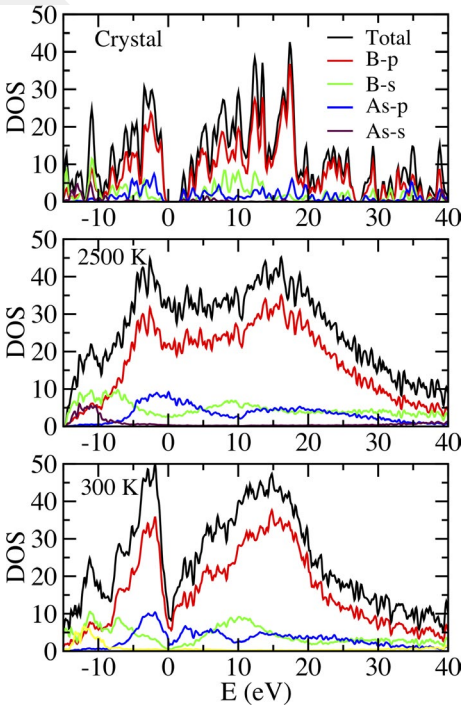

FIGURE 8 Total and partial density of states. The Fermi level is at 0 eV [Color figure can be viewed at wileyonlinelibrary.com]

comparable with the experimental value of 3.2-3.37 eV[20,21] and the previous theoretical data of 2.3-2.78 eV.[2,22–24] The liquid state presents a typical metallic behavior since it has the overlapped bands with no band gap. On the other hand, for the amorphous configuration, it is indeed hard to express whether it is metal or semiconductor because its TDOS does not show a clear band gap but a semimetallic-like band structure. From the inverse participation ratio,

$$\mathrm{IPR}\left(\psi_j\right) = N \sum_{i=1}^{N} a_i^{k4} \Bigg/ \left(\sum_{i=1}^{N} a_i^{k2} \right)^2$$

(where $\psi_k = \sum_{i=1}^{N} a_i^k \phi_i$ is the k^{th} eigenstate and N is the number of atoms) analysis given in Figure 9, a small bad gap of 0.3 eV is estimated for the amorphous configuration and the electron states near Fermi level are localized as typical for amorphous semiconductors. Consequently, we propose that the amorphous form presents a semiconducting nature but its band gap is significantly smaller than that of the crystal. This might be expected because amorphous B has a band gap energy ranging from 0.51 to 1.0 eV[25–28] and the crystalline and amorphous As are semimetal. From the IPR, for the liquid phase we see that the eigenvalues near Fermi Level (at 0 eV) overlap, its IPR has low values and hence the states are delocalized. These findings provide additional support its metallic character. From the PDOS provided in Figure 8, one can see that B-p state offers the main contributions to both valance and conduction bands. As-p states also provide some contributions to both bands near Fermi level. The contribution of As-s and B-s states near to Fermi level is insignificant.

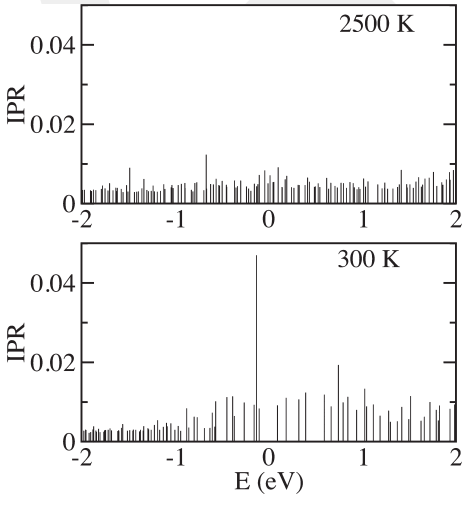

FIGURE 9 Inverse participation ratio at 2500 and 300 K. The Fermi level is at 0 eV

4 | DISCUSSION

The structural analyses reveal that the amorphous form of $B_{12}As_2$, in particular the environment of some of B-atoms, is partly parallel to the crystal. On the other hand, the liquid state of $B_{12}As_2$ is structurally very different from its solid amorphous and crystalline phases. The pentagonal pyramids hardly persist in the liquid form. The mean CNs in the liquid state are considerably less than those in the solid arrangements. We believe that this is mainly due to about 40% volume expansion in its liquid state. The volume selling also occurs in the amorphous form but it is rather small relative to the expansion seen in the liquid state. We need to point out here that the density of liquid $B_{12}As_2$ (2.46 g/cm^3) predicted is in reasonable limits considering the density of liquid boron (2.34-2.4 g/cm^3).[29,30]

The electronic structure examination exposes that the liquid state is metallic while the amorphous configuration is semiconducting with a band gap of 0.3 eV. Considering the electrical feature of liquid and amorphous B, these findings are also unsurprising because liquid B also shows a metallic behavior[31] while amorphous B is semiconducting. Note that B-p states mainly control the electronic structure of these materials and the semiconducting behavior is associated with the icosahedral arrangements. Also we believe that the formation of more As-As type configurations in the amorphous form also plays some role in the drastic closure of band gap energy, relative to the crystal.

5 | CONCLUSIONS

The atomic and electronic structures of the liquid and amorphous forms of $B_{12}As_2$ are, for the first time, revealed using ab initio MD simulations. About 40% volume enlargement is perceived for the melt and hence its local structure is significantly different from that of the crystal and amorphous states. The density of the liquid state is found to be close to that of liquid boron. In the liquid form at 2500 K, the mean CN of B and As atoms is 4.4 and 2.5, correspondingly. Such a large volume swelling is probably responsible for such a low mean coordination. As the temperature applied is gradually decreased, the volume gradually decreases and a glass-transition zone at around 1400 K is perceived. Amorphization leads to about 14% volume expansion. During the rapid solidification process, as expected, both average CNs steadily increase and reach values of 5.5 (B-atom) and 4.14 (As-atom) at room temperature. The pentagonal pyramid-like motifs hardly persist at 2500 K but during the rapid solidification procedure they grow gradually and some of which yield the formation of B_{12} molecules. In spite of the presence of the chain-like and A7-like As-As clusters in the amorphous configuration,

it is found to be partially similar to the crystalline crystalline $B_{12}As_2$ phase. The liquid structure exhibits a metallic character while the amorphous configuration presents a semiconducting nature having an energy band gap much smaller than that of the crystalline phase.

ACKNOWLEDGMENTS

This study was supported by the Scientific and Technological Research Council of Turkey (TÜBİTAK) under grant number 117M372. The simulations were run on the TÜBİTAK ULAKBİM, High Performance and Grid Computing Center (TRUBA resources).

ORCID

Murat Durandurdu https://orcid.org/0000-0001-5636-3183

REFERENCES

1. Emin D. Icosahedral boron-rich solids. Phys Today. 1987;40:55–62.
2. Morrison I, Bylander DM, Kleinman L. Bands and bonds of $B_{12}As_2$. Phys Rev B. 1992;45:1533–7.
3. Chu TL, Hyslop AE. Preparation and properties of boron arsenide films. J Electrochem Soc. 1974;121(3):412–5.
4. Emin D. Unusual properties of icosahedral boron-rich solids. J Solid State Chem. 2006;179:2791–8.
5. Cherednichenko KA, Le Godec Y, Solozhenko VL. Equation of state of boron subarsenide $B_{12}As_2$ to 47 GPa. High Pressure Res. 2018;38(3):224–31.
6. Pomeroy JW, Kuball M, Hubel H, Van Uden NW, Dunstan DJ, Nagarajan R, et al. Raman spectroscopy of $B_{12}As_2$ under high pressure. J Appl Phys. 2004;96:910–2.
7. Ovsyannikov SV, Polian A, Munsch P, Chervin JC, Le Marchand G, Aselage TL. Raman spectroscopy of $B_{12}As_2$ and $B_{12}P_2$ up to 120 GPa: evidence for structural distortion. Phys Rev B. 2010;81(14):140103–6.
8. Wu J, Zhu H, Hou D, Ji C, Whiteley CE, Edgar JH, et al. High pressure X-ray diffraction study on icosahedral boron arsenide ($B_{12}As_2$). J Phys Chem Solids. 2011;72:144–6.
9. Lee S, Bylander DM, Kleinman L. Elastic moduli of B_{12} and its compounds. Phys Rev B. 1992;45:3245–7.
10. Fan Z, Wang B, Xu X, Cao X, Wang Y. First-principles calculation of vibrational properties of $B_{12}As_2$ crystal. Phys Status Solidi B. 2011;248:1242–7.
11. Correia LA, Van Oort RC, Van der Put PJ. Chemical vapour deposition of boron subarsenide using halide reactants. React Solids. 1986;2:203–13.
12. Ordejón P, Artacho E, Soler JM. Self-consistent order-N density-functional calculations for very large systems. Phys Rev B. 1996;53:R10441–R10444.
13. Troullier N, Martins JL. Efficient pseudopotentials for plane-wave calculations. Phys Rev B. 1991;43:1993–2006.
14. Becke AD. Density functional exchange energy approximation with correct asymptotic behavior. Phys Rev A. 1988;38:3098–100.
15. Lee C, Yang W, Parr RG. Development of the Colle-Salvetti correlation-energy formula into a functional of the electron density. Phys Rev B. 1988;37:37785–9.
16. Le Roux S, Petkov V. ISAACS–interactive structure analysis of amorphous and crystalline systems. J Appl Crystallogr. 2010;43:181–5.
17. Momma K, Izumi F. VESTA 3 for three-dimensional visualization of crystal, volumetric and morphology data. J Appl Crystallogr. 2011;44:1272–6.
18. Morosin B, Mullendore AW, Emin D, Slack GA. Rhombohedral crystal structure of compounds containing boron-rich icosahedra. AIP Conf Proc. 1986;140:70–86.
19. Chiba A, Tomomasa M, Hayakawa T, Bennington SM, Hannon AC, Tsuji K. Pressure-induced suppression of the Peierls distortion of liquid As and Ge X (X= S, Se, Te). Phys Rev B. 2009;80:060201–4.
20. Bakalova S, Gong Y, Cobet C, Esser N, Zhang Y, Edgar JH, et al. Energy band structure and optical response function of icosahedral $B_{12}As_2$: a spectroscopic ellipsometry and first-principles calculational study. Phys Rev B. 2010;81:075114–3.
21. Klein PB, Nwagwu U, Edgar JH, Freitas JA Jr. Photoluminescence investigation of the indirect band gap and shallow impurities in icosahedral $B_{12}As_2$. J Appl Phys. 2012;112:013508-20.
22. Li D, Ching WY. Fundamental studies on the structures and properties of some B_{12}-based crystals. Phys Rev B. 1995;52:17073–83.
23. Gao F, Qin X, Wang L, He Y, Sun G, Hou L, et al. Prediction of new superhard boron-rich compounds. J Phys Chem B. 2005;109:14892–5.
24. Armstrong DR, Bolland J, Perkins PG. The electronic structure of α-B_{12}, $B_{12}P_2$ and $B_{12}AS_2$. Theor Chim Acta. 1984;64:501–14.
25. Hori A, Takeda M, Yamashita H, Kimura K. Absorption edge spectra of boron-rich amorphous films constructed with icosahedral cluster. J Phys Soc Jpn. 1995;64:3496–505.
26. Kimura K, Tada T, Hori A, Furukawa A. Optical absorption edge and photoluminescence spectra in amorphous and crystalline boron-rich solids. J Non-Cryst Solids. 1991;137:919–22.
27. Berezin AA, Golikova OA, Kazanin MM, Khomidov T, Mirlin DN, Petrov AV, et al. Electrical and optical properties of amorphous boron and amorphous concept for ß-rhombohedral boron. J Non-Cryst Solids. 1974;16:237–46.
28. Kuhlmann U, Werheit H, Lundström T, Robers W. Optical properties of amorphous boron. J Phys Chem Solids. 1994;55:579–87.
29. Millot F, Rifflet JC, Sarou-Kanian V, Wille G. High-temperature properties of liquid boron from contactless techniques. Int J Thermophys. 2002;23:1185–95.
30. Pape SL, Correa AA, Fortmann C, Neumayer P, Döppner T, Davis P, et al. Structure measurements of compressed liquid boron at megabar pressures. New J Phys. 2013;15:085011–9.
31. Vast N, Bernard S, Zerah G. Structural and electronic properties of liquid boron from a molecular-dynamics simulation. Phys Rev B. 1995;52:4123–30.

How to cite this article: Durandurdu M. Liquid and amorphous states of boron subarsenide. *J Am Ceram Soc*. 2020;103:176–182. https://doi.org/10.1111/jace.16720